Journal of Alloys and Compounds 509 (2011) 644–647

Contents lists available at ScienceDirect

Journal of Alloys and Compounds

journal homepage: www.elsevier.com/locate/jallcom

Characterization of the martensitic transformation in $Ni_{50-x}Ti_{50}Cu_x$ alloys through pure thermal measurements

Adelaide Nespoli*, Elena Villa, Stefano Besseghini

Consiglio Nazionale delle Ricerche – Istituto per l'Energetica e le Interfasi (CNR-IENI), U.O.S. di Lecco,Corso Promessi sposi 29, 23900 Lecco, Italy

ARTICLE INFO

Article history:
Received 6 April 2010
Received in revised form 30 August 2010
Accepted 1 September 2010
Available online 25 October 2010

Keywords:
Martensitic transformation
Orthorhombic
Monoclinic
NiTiCu
Electrical resistance

ABSTRACT

The addition of a third element to the Ni–Ti system often changes the product and the path of the martensitic transformation of the alloy, which is a direct B2–B19′ transformation for the NiTi alloy in the fully annealed state. In this study we investigate the martensitic transformation of fully annealed $Ni_{50-x}Ti_{50}Cu_x$ (x = 3–10 at%) shape memory alloy (SMA) samples using differential scanning calorimetry (DSC) and the four-probe electrical resistance (ER) measurements under stress-free conditions. DSC and ER data show that the ternary alloy goes through a direct B2–B19′ transformation for Cu content between 3 and 7 at% and through the two-stage B2–B19–B19′ transformation for Cu content between 8 and 10 at%. We find good agreement between the two techniques as regards the detection of the phase transformation temperatures. B19′ starting and finishing temperatures decreases with the increases of Cu content and show a significant reduction starting from 7 at%; the range of temperatures in which B19 is stable increases with increasing Cu content.

1. Introduction

The addition of a third element to the binary Ni–Ti system is often used to change the phase transformation temperatures. The great part of alloying elements lower the transformation temperatures as respect to the Ni–Ti system (as an example Cr, Mn, Fe, V, Co for Ni and Al for Ti). There are instead few elements which contribute to increase the transformation temperatures, as Zr for Ti and Au, Hf, Pt and Pd for Ni. A third element also alters the product of the martensitic transformation which is a direct B2–B19′ for NiTi. For example, adding Fe for Ni the alloy shows a two-stage B2–R–B19′ transformation, while with the substitution of Ni for Pd the transformation changes into B2–B19 (B2, B19′, R, B19 are the cubic, the monoclinic, the rombohedral and the orthorhombic structure, respectively) [1].

Ni–Ti–Cu ternary systems, where Cu substitutes Ni, have been largely studied from various aspects and many results are available. The addition of Cu for Ni reduces the sensitivity of the transformation temperatures to the chemical composition and to the thermal treatment time; diminishes the thermal hysteresis; reduces the mechanical hysteresis in the pseudoelastic regime; enhances the thermo-mechanical cycling stability [2].

It is well known [3,4] that $Ni_{50-x}Ti_{50}Cu_x$ alloys go through different sequences of martensitic transformation when Cu concentration is varied in some specific limits: ternary alloys containing up to 5–7 at% of Cu undergo through a B2–B19′ transformation; for Cu content belonging to the 7–16 at% range the ternary alloy shows the two-stage B2–B19–B19′ martensitic transformation; for Cu concentration higher than 16 at% the ternary alloy exhibits the B2–B19 transformation. Debates on the existence or not of the B19–B19′ transformation for x > 16 at% are still present in literature.

Under stress-free conditions, differential scanning calorimeter (DSC) and electrical resistance (ER) measurements represent two of the most common techniques used to analyze NiTi or NiTi-based systems in terms of detection of the phase transformation temperatures, analysis of the alloy structure and identification of the transformation path [4–11].

In this study we investigate the effect of Cu content (3–10 at%) on the path of the martensitic transformation in $Ni_{50-x}Ti_{50}Cu_x$ ternary alloys through the four-probe electrical resistance (ER) measurements and the differential scanning calorimetry (DSC) under stress-free conditions. Before starting ER measurements, we studied the influence of the electrical contact on the NiTiCu sample.

2. Materials and methods

$Ni_{50-x}Ti_{50}Cu_x$ (x = 3–10 at%) buttons were prepared by a non-consumable electrode vacuum arc furnace, Leybold LK6/45, under protective atmosphere. The elemental compositional analysis of each sample was carried out using an Energy Dispersive X-ray Spectrometer (EDS) INCA ENERGY 200 (Oxford Instruments) in connection with a scanning electron microscopy (SEM LEO 1430). Samples were then hot-rolled at 900 °C till a 3 mm of thickness, cut and then rolled to a 1 mm square section wire. The introduction of defects during the working phase stabilizes the B19 martensite and inhibits the nucleation of the B19–B19′ transformation [11]. As a con-

* Corresponding author. Tel.: +39 0341 499181; fax: +39 0341 499214.
E-mail address: a.nespoli@ieni.cnr.it (A. Nespoli).

0925-8388/$ – see front matter © 2010 Elsevier B.V. All rights reserved.
doi:10.1016/j.jallcom.2010.09.145

sequence, in order to detect the two-stage B2–B19–B19′ martensitic transformation we decided to test the samples in their orderly state, by fully annealing at 850 °C in vacuum for 1 h; the samples were then water quenched and electro-polished.

Resistance measurements were made using a Resistomat® 2305 device in the four-probe mode; each NiTiCu sample was immersed in a thermostatic bath (Lauda Ecoline RE306 with Kryo20 silicon oil) and subjected to four thermal cycles (from −35 °C to 100 °C), with a rate of 1 °C/min. Before starting electrical resistance measurements we studied three different ways of fixing the four electrical contacts to the NiTiCu wire: full-contact, screw and arc-welding modes, Fig. 1. With the full-contact mode the four electrical contacts are fixed in a well defined position on a thin plastic plate which is pushed against the SMA wire by two metallic springs; with the screw mode the four electrical contacts are screwed down to the SMA wire by four mini-clamps; with the arc-welding mode a 24 V electrical signal is use to spot-weld the electrical contacts to the SMA wire. The $Ni_{40}Ti_{50}Cu_{10}$ ER signals registered using the three contact modes are reported in Fig. 1.

The full-contact mode was immediately discarded as the registered ER signal refers to a portion of SMA wire length which continuously varies during the measurement, as the electrical contacts are fixed on the plastic plate instead being directly connected to the SMA wire; as a consequence the ER signal is visibly disturbed.

The tests conducted using the screw and the arc-welding modes give the same phase transformation temperatures which can be identified from the ER graph using the tangent method, but they show two different ER signals during the B2–B19 transformation, near 60 °C (highlighted by the grey line in Fig. 1). The enhancement observed using the screw mode is essentially due to the punctual load exerted by the screws, which provoke the growth of a localized stress induced martensite which in turn causes the ER intensification. The uncontrollable ER signal enhancement does not allow us to compare the ER measurements obtained from different samples, even though they turn out similar phase transformation temperatures. As a result of these considerations, the ER measurements were all conducted using the arc-welding mode.

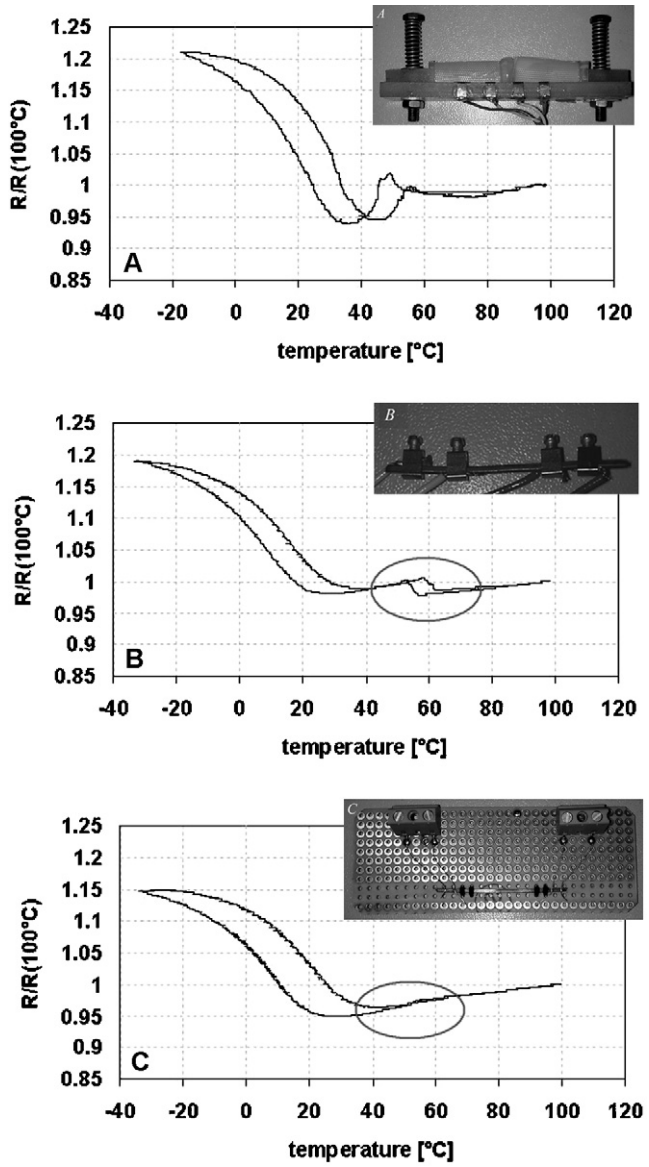

Fig. 1. ER signal derived from three modes of connecting the electrical wires to the NiTiCu sample. (A) Full-contact mode, (B) screw mode, (C) arc-welding mode.

The ER data were normalized to the length and to the section of the corresponding specimen in order to compare signals deriving from the eight different NiTiCu specimens.

DSC measurements were made using a Q100 TA Instruments device with liquid nitrogen cooling system. Each DSC measurement was conducted in the −50 °C to +100 °C range with a rate of 5 °C/min, and data were normalized to the sample weight.

In the two pure thermal analyses we used two different heating/cooling rates, 1 °C/min and 5 °C/min for ER and DSC measurements respectively. The heating/cooling rate may strongly affect the phase transformation temperatures, as Wang et al. [12] and Nurveren et al. [13] reported. Accordingly with this works, for low cooling rates the martensite starting and finishing temperatures do not show any marked variation. Moreover, a low cooling rate help us to easily detect the monoclinic transformation as the DSC signal referred to this phase transition is very low and would be confused with the base-line for high rate values. For this reason we expect to obtain similar and truthful results from the ER and DSC measurements.

Martensite transformation temperatures were extrapolated from ER and DSC graphs using the tangent method.

3. Results

Fig. 2 shows the ER data of each $Ni_{50-x}Ti_{50}Cu_x$ (x = 3–10 at%) sample overlapped to the DSC ones. As we can see from this figure the shape of the resistivity curves changes strongly depending on Cu content. For Cu < 7 at% the resistivity signal shows one minimum which corresponds to the B2–B19′ starting temperature, Ms. Two minima are observed for Cu belonging to the 8–10 at% range: the higher one corresponds to the B2–B19 starting temperature, Ms′, while the lower one to Ms. The separation between Ms′ and Ms increases with increasing Cu content, being 6.2 °C, 11.7 °C and 28 °C for the 8 at%, the 9 at% and the 10 at% Cu alloy respectively. We can also observe that during the B2–B19′ and the B19–B19′ transformations resistivity increases with increasing Cu content; a very low variation, about 1 μΩ cm, is instead registered during the B2–B19 one.

DSC curves strongly change depending on Cu content. One clear peak is observed on cooling representing the B2–B19′ and the B2–B19 transformations for Cu content below 7 at% and higher than 8 at% respectively. These latter alloys present a second spread peak representing the B19–B19′ transformation. The enthalpy associated to the martensitic transformation varies as a function of the Cu content and is in a strict relationship with the alloy structure; from the DSC data we estimated 35 J/g, 17 J/g and 4 J/g during the B2–B19′, B2–B19 and the B19–B19′ transformation respectively. The 8 at% Cu alloy does not show a clear separation between the B2–B19 and the B19–B19′ transformation as the ER and the DSC signals do not show two visible separated minima and peaks respectively.

The characteristic martensitic starting and finishing temperatures, Ms′, Mf′, Ms and Mf, estimated from the two techniques are reported in Fig. 3 as a function of Cu content; the existing areas associated to the B2, B19 and B19′ structures derived from DSC and ER analysis are reported as well. The two techniques give similar results. In particular, we can see that the monoclinic starting and finishing temperatures, Ms and Mf, have a similar trend, decreasing with increasing Cu content and have a significant reduction starting from 7 at%. As opposite, Ms′ and Mf′ raise when Cu content is increasing; the range of temperature in which B2 transforms into B19 is very short and is about constant by increasing Cu content, being equal to 10 °C when Cu is varied in the 8–10 at% range. The temperature range over which the B19 is stable becomes wide with increasing Cu content.

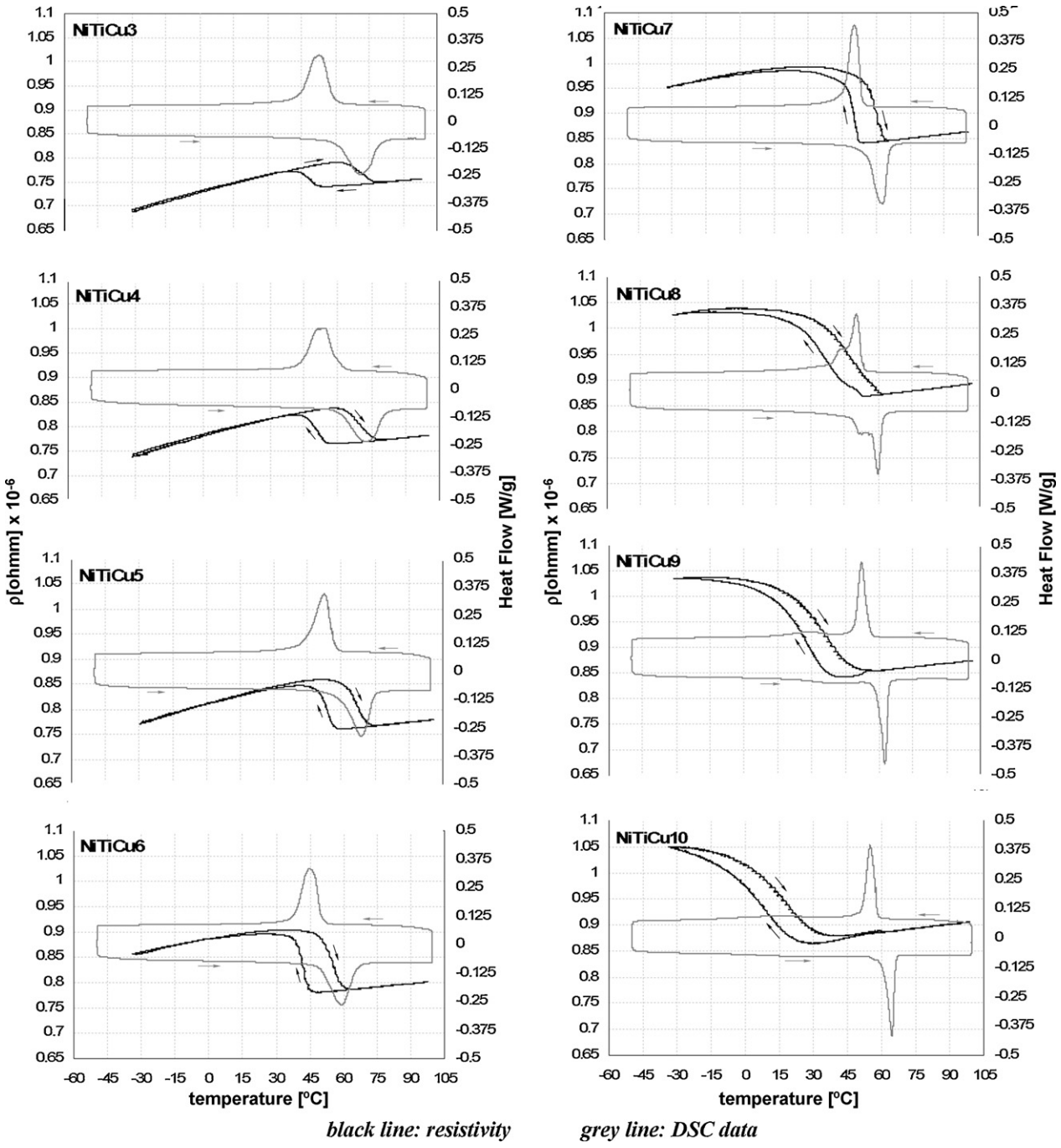

Fig. 2. ER and DSC measurements. Comparison between the resistivity (black lines) and the differential scanning calorimeter (grey lines) data of the $Ni_{50-x}TiCu_x$ (x = 3–10 at%) samples.

4. Discussions

ER and DSC measurements were conducted in order to study the martensitic path and the phase transformation temperatures in $Ni_{50-x}TiCu_x$ (x = 3–10 at%) samples. The two techniques give an identical result as regards the identification of the martensitic product and path. There are two different ER and DSC trends depending on Cu content. According to literature [1–4,8], we associate to the DSC cooling peak and to the ER cooling minimum the B2–B19′ transformation when Cu content is below 7 at%; when Cu is varied in the 8–10 at% range, we relate to the first DSC cooling peak and to the first almost invisible ER cooling change the B2–B19 transformation and to the second DSC cooling peak and to the second ER cooling minimum the B19–B19′ transformations.

DSC and ER techniques provide two main information: DSC gives prominence to the B2–B19 transformation while ER measurement supplies for a higher B19–B19′ signal. This complementary behavior can be explained based on the results published by Nam et al. [4], Lo et al. [8], Morberly et al. [14] and Saburi et al. [15]: the energy associated to the nucleation and to the martensite growth and propagation in the B2–B19 transformation is higher than the one related to the monoclinic distortion of B19 into B19′. This fact explains the maximum peak registered in the DSC measurement during the transformation from B2 into B19 or B19′ and the diffuse and almost indiscernible peak associated to the B19–B19′ transformation. As opposite, the B2–B19 transformation shows a small ER variation; the main ER signal derives from the B2–B19′ and the B19–B19′ transformations. This behavior is related to the fact that

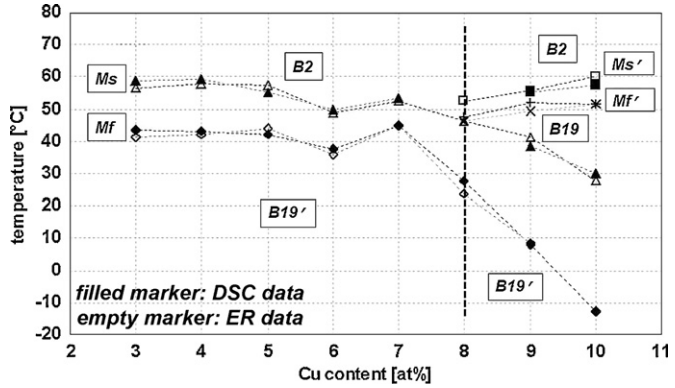

Fig. 3. Martensitic transformation temperatures. Ms (triangular markers), Mf (rhombus markers), Ms′ (square markers) and Mf′ (cross markers) temperatures of the $Ni_{50-x}TiCu_x$ samples as a function of Cu content derived from the ER (empty markers) and the DSC (filled markers) data; B2, B19′ and B19 regions are pointed out.

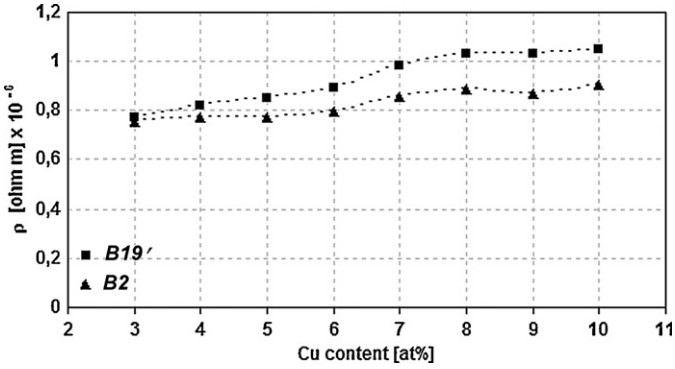

Fig. 4. B2 and B19′ resistivity registered at Af and Mf temperatures respectively.

no lattice invariant shear is required for the B2–B19 transformation. B19 appears as a twinless and a defect-free martensite. As the crystal structure, deformation defects, accommodated twin variants and crystal distortion contribute to the ER signal enhancing, we can assert that the contribution to the high resistance value we obtained on B19–B19′ and on B2–B19′ origins from the internal strain effects, the twinning, and from the distortion of the beta angle.

For both ER and DSC measurements the orthorhombic structure becomes clear when Cu content is higher than 8 at%. The characteristic starting temperatures, Ms, Mf, Ms′ and Mf′ are presented in Fig. 3 as a function of Cu content. Ms and Mf temperatures decrease when Cu content increases; this phenomenon is much evident for Cu content higher than 8 at%, where orthorhombic phase is also present. As opposite, Ms′ and Mf′ temperatures increase with increasing Cu content.

In order to evaluate the influence of the crystalline structure on the resistivity signal, we compare the B2 and B19′ resistivity registered at Af and Mf temperature of each NiTiCu sample, see Fig. 4. We can note the B2 resistivity varies between the 80–90 μΩ cm and is always lower than the B19′ one which changes within 80–100 μΩ cm limits. In this graph we can also notice two important behaviors. First, B2 and B19′ resistivity shows three different trends: for Cu content between 3 and 5 at% B19′ resistivity is almost constant and is nearly equal to B2 one; for Cu content between 5 and 7 at% B2 and B19′ resistivity increases with two different rates; for Cu content between 7 and 10 at% B2 and B19′ resistivity is approximately constant. This behavior may suggest that the change of transformation mode from B2–B19′ to B2–B19–B19′ occurs when Cu content varies between 5 and 7 at% and not at 8 at% as DSC and the direct ER measurements show (Fig. 2). This behavior is confirmed by the Ms and Mf temperature which show a constant trend between 3 and 5 at% and a significant reduction after 7 at% (Fig. 3).

A second interesting phenomenon is related to the transformation path which seems to influence the B19′ resistivity which is almost equal to the B2 one when B19′ is created by B2–B19′ and increases when B19′ originates through B2–B19–B19′. At present we are studying these phenomena through new experiments.

5. Conclusions

In this work we present the four-probe electrical resistance measurements and the differential scanning calorimetry analysis of $Ni_{50-x}TiCu_x$ (x = 3–10 at%) samples, in order to study the path and the transition temperatures of the martensitic transformation under stress-free condition. We find that the alloys go through a B2–B19′ transformation when Cu content is below 8 at% and to the B2–B19–B19′ path when Cu belongs to the 8–10 at% range. A deep investigation on resistivity signal suggests that the B2–B19–B19′ transformation may originate starting from 7 at%. We find good agreement between the two techniques as regards the detection of the phase transformation temperatures. The two methods result to be complementary one with the other as regard the evaluation of the path of the martensitic transformation: ER measurement results to be more sensitive in the evaluation of the B19–B19′ transformation and DSC measurement reveals to be more responsive of the B2–B19 transformation.

References

[1] K. Otsuka, X. Ren, Progress in Materials Science 50 (2005) 511–678.
[2] H. Funakubo, Shape Memory Alloys, Gordon & Breach Science Publishers, 1984.
[3] T.H. Nam, T. Saburi, Y. Nakata, K. Shimizu, Materials Transactions JIM 31 (1990) 1050–1056.
[4] T.H. Nam, T. Saburi, K. Shimizu, Materials Transactions JIM 31 (1990) 959–967.
[5] A.S. Paula, K.K. Mahesh, Materials Science and Engineering A 481–482 (2008) 146–150.
[6] V. Antonucci, G. Faiella, M. Giordano, F. Mennella, L. Nicolais, Thermochimica Acta 462 (2007) 64–69.
[7] H. Matsumoto, Physica B 190 (1993) 115–120.
[8] Y.C. Lo, S.K. Wu, H.E. Horng, Acta Metallurgica et Materialia 41 (3) (1993) 747–759.
[9] J. Uchil, K.P. Mohanchandra, K. Ganesh Kumara, K.K. Mahesh, Materials Science and Engineering A 251 (1998) 58–63.
[10] S.K. Wu, H.C. Lin, T.Y. Lin, Materials Science and Engineering A 438–440 (2006) 536–539.
[11] K. Tsuji, K. Nomura, The influence of cold working on transformation properties of Ni–Ti–Cu alloys, Scripta Metallurgica et Materialia (1990) 2037–2042.
[12] Z.G. Wang, X.T. Zu, Y. Huo, Thermochimica Acta 436 (2005) 153–155.
[13] K. Nurveren, A. Akdoğan, W.M. Huang, Journal of Materials Processing Technology 196 (2008) 129–134.
[14] W.J. Morberly, J.L. Proft, T.W. Duerig, R. Sinclair, Materials Science Forum 56–58 (1990) 605–610.
[15] T. Saburi, Y. Watanabe, S. Nenno, ISIJ International 29 (5) (1989) 405–411.